# Paleoaltimetry incorporating atmospheric physics and botanical estimates of paleoclimate

**Chris E. Forest*** *Department of Earth, Atmospheric, and Planetary Sciences, Massachusetts Institute of Technology, Cambridge, Massachusetts 02139*

**Jack A. Wolfe** *Department of Geosciences, University of Arizona, Tucson, Arizona 85745*

**Peter Molnar**, **Kerry A. Emanuel** *Department of Earth, Atmospheric, and Planetary Sciences, Massachusetts Institute of Technology, Cambridge, Massachusetts 02139*

## ABSTRACT

**We present a method for deducing paleoaltitudes that incorporates basic physical principles of atmospheric science and inferences of paleoclimates from plant leaf physiognomy. We exploit the average west-to-east flow of the atmosphere at mid-latitudes and a thermodynamically conserved variable in the atmosphere—moist static energy (the combined internal, latent heat, and gravitational potential energy of moist air)—to develop a method that relies on a parameter that varies with height in the atmosphere in a predictable fashion. Because the surface distribution of moist static energy is constrained by atmospheric dynamics and thermodynamics, the combined internal and latent heat energies, also known as the moist enthalpy, should only vary with altitude provided we know the distribution of moist static energy. Thus, we avoid having to make assumptions about the mean annual temperature lapse rate, which varies spatially and temporally owing to unpredictable variations in atmospheric water vapor. To estimate a paleoaltitude, therefore, we require (1) a priori knowledge of the spatial distribution of moist static energy for the paleoclimate and (2) the ability to estimate paleoenthalpy for two isochronous locations: one at sea level, the other at some unknown elevation. To achieve this, we investigated the spatial distribution of moist static energy for the present-day climate of North America to estimate the deviations in moist static energy from zonal invariance. In parallel, we quantified the relation between moist enthalpy and plant leaf physiognomy of modern forests. Assuming that such deviations from zonal invariance and such relationships between physiognomy and enthalpy apply to ancient climates and fossil leaves, these investigations yield an uncertainty estimate of ±910 m in the paleoaltitude difference between two isochronous fossil assemblage locations.**

## INTRODUCTION

More than 50 yr of research have demonstrated the need for accurate estimates of paleoelevations in the fields of geophysics, paleoclimatology, and paleobotany. Rapid (~1 mm/yr) vertical motions of large tracts of the Earth's surface over periods of 1 m.y. or more appear to require dynamic processes in the mantle (e.g., England and Houseman, 1989), and therefore a knowledge of elevation changes should place a bound on such dynamic processes. Moreover, high plateaus force atmospheric circulations (e.g., Webster and Chou, 1980; Held, 1983; Murakami, 1987; Young, 1987; Trenberth and Chen, 1988), implying that changes in their elevations may have influenced not only local, but even global climate changes throughout history (e.g., Ruddiman and Raymo, 1988; Ruddiman and Kutzbach, 1991; Raymo and Ruddiman, 1992). Paleobotanical evidence offers the most direct indication of paleoclimatic changes in continental regions, but clearly many ecological conditions vary similarly with latitude and altitude. Correspondingly, to exploit all climate information from a fossil assemblage, the component of climate relating to local or regional elevation must be determined. Thus, the paleobotanical record on both local and global scales, the climate changes of both local and global scales, and the evolution of mean elevations of large tracts of land should be closely linked. Calculating elevation from climate variables requires measuring an atmospheric quantity that varies with altitude, such as paleopressure or paleotemperature. Most attempts to estimate paleoelevation have exploited fossil evidence implying temperature differences, but recent results show that paleopressures can be estimated, if with relatively poor accuracy. Two such methods are discussed in the Appendix. One is derived from basalt vesicularity and the other from measured cosmogenic nuclide concentrations.

Estimating paleotemperatures has been more successful than estimating paleopressures for determining paleoaltitudes. Mean temperatures show correlations with leaf morphology of living plant assemblages with uncertainties in mean annual temperature perhaps as small as 1 °C (Wolfe, 1979, 1993). Hence, assuming that foliar characteristics of leaf fossil assemblages obey the same relationships, we should be able to infer correspondingly accurate paleotemperatures. Because temperature varies with latitude, longitude, and elevation, and because temperature has varied over geologic time, the calculation of paleoelevation from paleotemperature involves comparing the surface temperature of a high-altitude location to that of a low-altitude location at the same latitude and of the same age (Axelrod, 1966). Hence, the use of paleobotanical data for paleoaltimetry consists of two steps: first, estimating a climatic parameter, like mean annual temperature, from fossil plants, and second, using differences in that parameter from separate sites to estimate elevation differences, given a priori knowledge of the variation of the parameter with altitude.

Two approaches to inferring paleoclimates from fossil plants have distinct philosophical

*E-mail: ceforest@mit.edu.

*GSA Bulletin*; April 1999; v. 111; no. 4; p. 497–511; 12 figures; 6 tables.

bases. Axelrod (1966) and Axelrod and Bailey (1969) suggested that taxonomic similarities between floral fossil assemblages and present-day forests could be used to infer paleoclimates. Each fossil taxon is assigned a nearest living relative defined at the species level when possible. Then, the climatic parameter of a present-day forest containing as many nearest living relatives of the floral assemblage as possible is assigned to the paleoclimate of the fossil locality. As others have noted (Wolfe, 1971; Meyer, 1986; Wolfe and Schorn, 1989; Chaloner and Creber, 1990; Gregory, 1994), this relies heavily on the assignment of genus and sometimes species to extinct plants, for which, in most cases, the fossil record includes only one plant organ that may not even be taxonomically significant. Thus, this assignment is heavily biased by living organisms with similar organs and makes the untested assumption that these organs indicate the sensitivity of both fossil and present-day plants to the relevant environmental characteristics, in this case temperature. Because separate organs of plants can evolve differently in changing environments, this assumption is tantamount to either (1) assuming that nature has fortuitously left a record of only those plant organs sensitive to climate change or (2) ignoring evolution. This assumption can be avoided if physiognomic characteristics of plants are used to infer local climates. Much work has shown that relationships exist between foliar characteristics and various climate parameters (Bailey and Sinnot, 1915, 1916; Wolfe, 1979, 1993; Gregory and Chase, 1992; Gregory, 1994), indicating that the latter approach is more useful and appropriate.

Heretofore, estimating elevation from differences in climatic parameters has been accomplished using empirical relationships between altitude and temperature derived from the present climate (the terrestrial lapse rate discussed in the following). Such relationships lack a firm theoretical basis, and the change in present-day surface temperatures with altitude in the western United States shows large spatial variations (Meyer, 1986, 1992; Wolfe, 1992). Moreover, we have no reason to expect that such laterally varying empirical relationships should hold in the different climates that have prevailed in geologic time. We therefore seek an inferable thermodynamic quantity, the distribution of which with altitude and longitude is well constrained by both theory and observation. The use of a quantity derived from fundamental thermodynamic laws is obviously more reliable than one fit empirically to data spanning a fraction of the twentieth century — a small fraction of geologic history. The remainder of this paper addresses such a quantity and develops its use as a paleoaltimeter. Wolfe et al. (1997) implemented this method in their paleoaltitude estimates for western North America during Miocene and Eocene times.

TABLE 1. TABLE OF SYMBOLS

| Symbol | Name | SI units |
|---|---|---|
| $c'_p$ | Specific heat capacity of moist air | J/kg/K |
| $c_{pd}$ | Specific heat capacity of dry air | J/kg |
| $c_{pv}$ | Specific heat capacity of water vapor | J/kg |
| $c_w$ | Specific heat capacity of liquid water | J/kg |
| $e$ | Vapor pressure | hPa |
| $e^*$ | Saturation vapor pressure | hPa |
| $g$ | Gravitational acceleration | J/m/kg |
| $G$ | $T + \gamma_t$ | K |
| $h$ | Moist static energy | J/kg |
| $h^*$ | Saturation moist static energy | J/kg |
| $H$ | Moist enthalpy | J/kg |
| $L_v$ | Latent heat of vaporization | J/kg |
| $L_{vo}$ | Latent heat of vaporization at 0 °C | J/kg |
| $p$ | Pressure | J/m$^3$ |
| $q$ | Specific humidity | g/kg |
| $q^*$ | Saturation specific humidity | g/kg |
| $R_v$ | Gas constant for water vapor | J/kg/K |
| $R_d$ | Gas constant for dry air | J/kg/K |
| $RH$ | Relative humidity | % |
| $T$ | Temperature | K |
| $T_d$ | Dew-point temperature | K |
| $Z$ | Altitude | m |
| $\gamma_t$ | Terrestrial lapse rate | K/m |
| $\varepsilon$ | Ratio of dry air to water vapor gas constants | |
| $\lambda$ | Eigenvalue | |
| $\rho_v$ | Water vapor density | kg/m$^3$ |
| $\sigma_i$ | Standard error of variable i | |

TABLE 2. VARIATIONS IN MOIST STATIC ENERGY COMPONENTS

| Parameter | Range | Energy component | Range |
|---|---|---|---|
| Temperature, $T$ | 0–30 °C | Specific heat, $c'_pT$ | 0–30 kJ/kg |
| Specific humidity, $q$ | 0–20 g/kg | Latent heat, $L_vq$ | 0–50 kJ/kg |
| Elevation, $Z$ | 0–4000 m | Gravitational potential, $gZ$ | 0–40 kJ/kg |

## Using Moist Static Energy

Two conservative thermodynamic variables commonly used in atmospheric physics are moist static energy and equivalent potential temperature, each derived from the first law of thermodynamics (e.g., Wallace and Hobbs, 1977; Emanuel, 1994). Moist static energy (per unit mass), the sum of moist enthalpy and gravitational potential energy per unit mass, is the total specific energy content of air, excluding kinetic energy, which is very small (<< 1%) compared with the other terms (Peixoto and Oort, 1992). Moist static energy, $h$, is written

$$h = c'_pT + L_vq + gZ = H + gZ \qquad (1)$$

where $c'_p$ is the specific heat capacity at constant pressure of moist air, $T$ is temperature (in K), $L_v$ is the latent heat of vaporization for water, $q$ is specific humidity , $g$ is the gravitational acceleration, $Z$ is altitude, and $H$ is moist enthalpy (symbols are listed in Table 1). We use the specific heat capacity of moist air, $c'_p = c_{pd}(1–q) + c_wq$, to account for compositional changes of the air, where $c_{pd}$ and $c_w$ are the specific heat capacities of dry air and liquid water, respectively. For consistency, we must also account for the temperature dependence of the latent heat of vaporization, $L_v + L_{vo}(1+(T–273)(c_{pv}–c_w))$, where $c_{pv}$ is the specific heat capacity at constant pressure of water vapor and $L_{vo}$ is the latent heat of vaporization at 0 °C. These second-order effects are most important in warm and moist climates, where they contribute variations of ~5–10 kJ/kg, which, if ignored, would introduce errors in inferred elevation of 500–1000 m.

Moist static energy is changed only by radiative heating and surface fluxes of latent and sensible heat, and, like equivalent potential temperature, is virtually conserved following air parcels. We consider only moist static energy because the relationship between altitude and equivalent potential temperature is less simple and direct. Considering the conservative properties of $h$, we note that typical variations in its components are roughly of equal magnitudes (Table 2).

Two properties of moist static energy make it a desirable candidate for inferring paleoelevations. First, it is nearly conserved following air parcels and hence is approximately constant along tra-

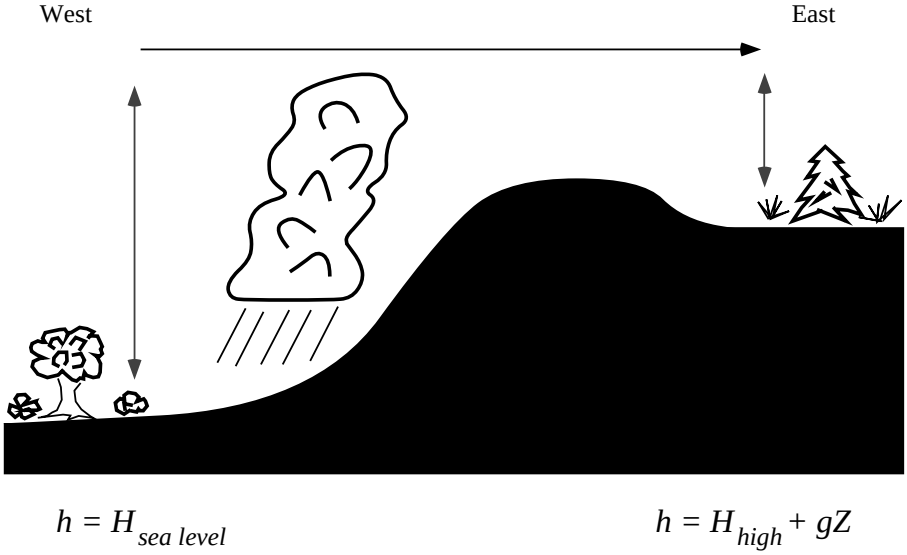


**Figure 1. Surface air conserves moist static energy as it traverses a mountainous region by converting between internal heat, latent heat, and potential energy. The potential energy for the high-elevation site is the difference in moist enthalpies, $H_{sea\ level} - H_{high}$, which yields the elevation estimate. The vertical arrows indicate the maintenance of the moist static energy profile by convective transports. The horizontal arrow indicates the typical west-to-east flow in the upper troposphere.**

jectories. Second, the value of $h$ in the boundary layer is usually strongly constrained by convection to be nearly equal to the value of $h$ in the upper troposphere. Owing to the Earth's rotation, air in the middle latitude upper troposphere flows nearly from west to east, so that contours of $h$ there should also extend approximately west-east. This implies that $h$ at the surface should be nearly invariant with longitude. We test this inference of longitudinal invariance later.

Assuming that $h$ is invariant with longitude along the Earth's surface, if we can estimate enthalpy at sea level ($H_{sea\ level}$) for a particular latitude, it follows from (equation 1) that the altitude of another location at the same latitude is given by

$$Z = \frac{H_{sea\ level} - H_{high}}{g}, \qquad (2)$$

where $H_{high}$ is the enthalpy at the high-altitude location (see Fig. 1).

In summary, the necessary assumptions to estimate paleoaltitude are that the surface moist static energy is invariant with longitude and that the moist enthalpy is a measurable quantity for the regional paleoclimate. The remainder of this paper tests these two assumptions and quantifies each error source.

## Moisture Parameter Definitions

We briefly review the basic definitions of specific humidity, relative humidity, and dew-point temperature to clarify the calculations of each from data (see Wallace and Hobbs, 1977, Emanuel, 1994, for derivations of formulas). Humidity variables are derived either from the density of water vapor, $\rho_v$, or, equivalently, from the vapor pressure, $e$, which are related through the ideal gas law, $e = \rho_v R_v T$ where $R_v$ is the gas constant for water vapor. The saturation vapor pressure, $e^*$, depends only on temperature and can be calculated using Bolton's (1980) empirical formula,

$$e^*(T) = 6.112 \exp\left(\frac{17.67T}{243.5 + T}\right) \qquad (3)$$

[in hPa with $T$ in °C], and is used to relate dew-point temperature, $T_d$, to ambient air temperature through relative humidity, $RH$, defined as

$$RH = \frac{e^*(T_d)}{e^*(T)} \qquad (4)$$

Dew-point temperature is the temperature to which the air must be cooled at constant pressure to achieve saturation, implying that vapor pressure is calculated via $e(T) = e^*(T_d)$. Specific humidity, $q$, the ratio of air's partial density of water vapor to the total density of moist air, is calculated via

$$q = \varepsilon \frac{e}{p - (1 - \varepsilon)e}$$

where $p$ is total pressure which, if necessary, can be calculated from elevation, and $\varepsilon = 0.622$, the ratio of gas constants for dry air and water vapor. Thus, if we know $p$, we can calculate $q$, provided that we can estimate the mean vapor pressure. Mean vapor pressure can be calculated either from an average value of $T_d$ using equation 3 or using average values of $T$ and $RH$ using equation 4.

## Spatial Distribution of Moist Static Energy

**Theoretical Constraints.** Before testing the assumption of longitudinal invariance, we discuss several meteorological constraints on the distribution of $h$. Particularly, we consider three processes, each affecting $h$ differently: (1) boundary layer convection, (2) free atmosphere convection, and (3) large-scale horizontal motions. The interaction of these atmospheric dynamic processes constrains moist static energy to be longitudinally invariant.

First, we consider convection in an unsaturated atmospheric boundary layer, approximately the lowest 1 km of the atmosphere. Boundary layer convection maintains a dry adiabatic vertical temperature gradient (lapse rate) which is $g/c_{pd}$ = 9.8 K/km. Hence, $c_{pd}T + gZ$ is essentially constant with altitude in the boundary layer. Moreover, the concentration of tracers is well mixed in such layers, implying that $q$ should be invariant with altitude in this layer (see Fig. 2). Thus $h$ should be nearly constant with altitude, a result confirmed by observations (Stull, 1989). This allows us to write

$$h_{surface} \cong h_{topBL}, \qquad (5)$$

where $h_{surface}$ is the value of $h$ at the Earth's surface and $h_{topBL}$ is the value of $h$ at the top of the boundary layer (BL).

Above the atmospheric boundary layer, the vertical temperature gradient is often close to its moist adiabatic value (Betts, 1982; Xu and Emanuel, 1989), implying the near invariance with height of the saturation moist static energy:

$$h^* = c_p' T + L_v q^* + gZ, \qquad (6)$$

where $q^*$ is the saturation specific humidity. Unlike $q$, $q^*$ is a state variable (i.e., a function of temperature and pressure alone). Now suppose a sample of air is displaced upward from the boundary layer far enough that the cooling makes it saturated; its value of $h$ will also be its value of $h^*$. Comparing the air sample's value of $h$ to the value of $h^*$ in the immediate environment is equivalent to comparing its temperature with that of its environment. If we neglect the small dependence of density on water substance in the sample, the buoyancy of the sample is a function of $T$, which directly determines $h^*$ at a given altitude. Thus, the vertical profile of $h^*$ indicates the buoyancy of vertically displaced air parcels. The frequently ob-

served neutral state for moist convection is thus characterized by $\partial h^*/\partial Z \cong 0$. In addition, the climatic value of $h$ at the bottom of the free atmosphere is constrained to be the climatic value of $h^*$. If $h_{topBL} > h^*_{topBL}$ the atmosphere would be unstable to convection. If $h_{topBL} < h^*_{topBL}$, surface heating and boundary layer convection would raise $h_{topBL}$ until convection occurs throughout the troposphere. For climatic time scales, the equilibrium between free atmosphere convection and surface heating results in the statement $h_{topBL} \approx h^*_{topBL}$. Because the vertical profiles are continuous, we can also write $h_{topBL} \approx h^*_{botFA}$ where $h^*_{botFA}$ is the value of the saturation moist static energy at the bottom of the free atmosphere (FA).

We recognize that for mid-latitudes, this approximation is true along surfaces of constant angular momentum, rather than strictly along the vertical direction, but these surfaces are nearly vertical. In the high troposphere the absolute temperature is small and $q = q^* \approx 0$. Therefore, at these altitudes, $h \approx h^*$. These constraints allow us to write

$$h_{surface} \cong h_{top}, \tag{7}$$

where $h_{top}$ is the value in the upper troposphere (Fig. 2).

Aside from convective constraints on $h$, we expect $h$ to be nearly longitudinally invariant in the upper troposphere. This results from the conservative property of $h$ along trajectories and from the generally west to east winds at these high altitudes. Dynamical constraints require that basic flow properties vary only over horizontal scales greater than about 1000 km, the Rossby radius of deformation in the middle-latitude troposphere (see Holton, 1992). We assume that radiative cooling will not affect the distribution of $h$ because the time scale to reach thermal equilibrium is much longer than that associated with transport across the continent. In summary, since $h$ should not vary rapidly with longitude in the upper troposphere and $h^*$ is nearly equivalent to $h$ there, and since $h^*$ is constrained to equal $h$ in the boundary layer by the condition of moist convective neutrality, $h$ within the boundary layer (and thus at the surface) should be approximately invariant with longitude.

**Surface Observations of Moist Static Energy.** To test the assumption of longitudinal invariance of moist static energy at least in the present climate, we used the observed distribution of $h$ across the North American continent. We calculated climatic values of $h$ from various climatic parameters that the National Climatic Data Center has listed in the International Station Meteorological Climate Summary (ISMCS), which is available on CD-ROM (National Climate Data Center, 1989). This data set provides annual mean values and means for each month for the variables listed in Table 3.

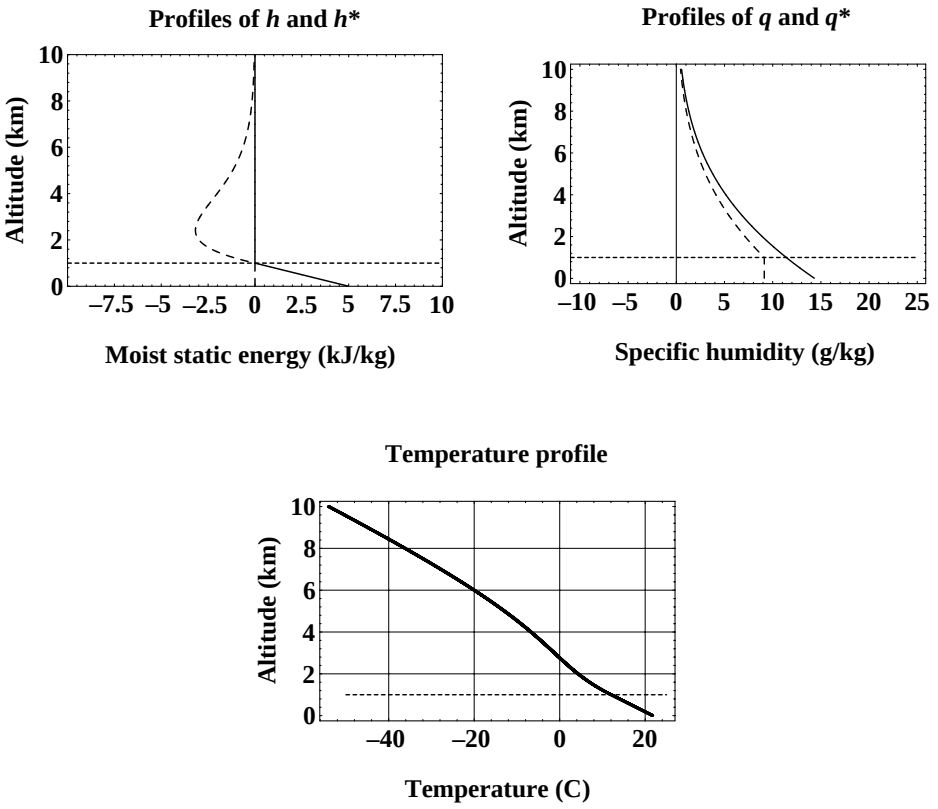


**Figure 2. We show schematic vertical profiles $h$ (dashed) and $h^*$(solid) in the left panel and $q$ (dashed) and $q^*$ (solid) in the right panel. The temperature profile (bottom), corresponding to $c^t_p T = h - gZ - L_v q$, illustrates the constant lapse rate within the boundary layer and the reduced lapse rate above the boundary layer. We chose the boundary layer depth to be 1 km and indicate it by the horizontal dashed line in each panel. These profiles illustrate typical climatic values that are determined by moist convective adjustment in the free atmosphere and dry adiabatic convection in the boundary layer.**

We calculated a mean moist static energy at each station, for which the altitude is known, by independently calculating a mean temperature and mean specific humidity (as described herein) and by combining the respective sensible, latent, and potential energies. We used averaging periods ranging from seasons to 1 yr and various formulations of mean temperature and mean specific humidity. Three classes of monthly averages were calculated for temperature and specific humidity: class one from daily maxima, class two from daily minima, and class three from daily means. The first two specific humidities were calculated from averages of daily relative humidity measurements taken at a given local standard time (LST). Calculating a specific humidity in this manner (using equations 3 and 4) requires an average temperature taken here as the corresponding average daily maximum or average daily minimum temperature. The third mean specific humidity was calculated from a monthly average of the daily mean dew-point temperature to correspond with the daily mean temperature. A mean $h$ is then calculated using temperature and specific humidity from these classes of monthly means: daily maximum values, daily minimum values, and daily mean values.

A moist static energy calculated from mean temperatures and humidities over a period is not necessarily equal to the mean moist static energy for that period. Because saturation vapor pressure is a nonlinear function of temperature, the mean vapor pressure is not equal to the vapor pressure calculated from the mean temperature. To estimate the effect of this nonlinear dependence, we took a subset of data and calculated mean specific humidity in two ways: from the mean vapor pressures and from the vapor pressure calculated from the mean dew-point temperature. We found that the average difference in specific humidity is 0.1 g/kg. This difference

TABLE 3. AVAILABLE CLIMATE DATA FROM ISMCS CD-ROM*

| Mean variable | Symbol | Record length (yr) | Number of stations |
|---|---|---|---|
| Maximum daily temperature | $T_{max}$ | ~30 | 699 |
| Minimum daily temperature | $T_{min}$ | ~30 | 699 |
| Daily temperature | $T_{mean}$ | ~30 | 699 |
| Daily dew-point temperature | $T_d$ | ~30 | 699 |
| Relative humidity at 6 or 7 LST† | *RH7* | ~10 | 238 |
| Relative humidity at 13 or 16 LST | *RH16* | ~10 | 238 |
| Daily vapor pressure | *e* | ~10 | 238 |

*NCDC, 1989.
†Local standard time.

translates to an error in altitude of 25 m, which is small compared to 910 m, the total expected error discussed in the following.

To examine the zonal variability of *h*, we first examined the spatial distribution on maps (Figs. 3, 4, and 5). The winter and summer means of *h* deviate from longitudinal invariance much more than spring, autumn, and annual means, but all show similarities to large-scale circulation patterns (Oort, 1983), as expected. A method to estimate this pattern for paleoclimates would provide a first-order correction to the assumption of zonal invariance. However, this requires predicting stationary waves for the paleoclimate setting, which is a current topic of research.

We quantified the longitudinal variability by statistically fitting *h* to monotonic functions of latitude, φ. Because we have tested for invariance, the standard deviation from the function is more important than the actual function. We fitted the mean values of *h* to a cubic function of φ using a standard least squares technique (Table 4) (see Fig. 3). As expected, winter and summer means show the largest deviations. Autumn exhibits the smallest deviations. We do not expect plant characteristics to correlate with mean autumn enthalpy, when photosynthesis and plant growth are minimal. Because foliar physiognomic character states correlate with mean annual temperature, we expect them to correlate with mean annual enthalpy. If one season revealed markedly smaller zonal variation, we would have investigated the correlations of climatic parameter in that season with foliar physiognomy, but from Table 4, we note that no seasonal deviation appears significantly better than the mean annual case. For the mean annual values, the standard deviation from zonal invariance of *h* is 4.5 kJ/kg (see Table 4). Dividing 4.5 kJ/kg by *g* yields a minimum estimate of the error in altitude of 460 m.

**Moist Static Energy vs. Mean Annual Temperature.** The focus of the previous section was to estimate the expected error from assuming the zonal invariance of mean values of moist static energy. This expected error contributes to the total expected error of a paleoaltitude estimate. Before proceeding to the next section (inferring paleoclimate from plant fossils), we examine the zonal invariance assumption as applied in the mean annual temperature approach to paleoaltimetry. Based on the initial method of Axelrod (1966), paleoaltitudes can be estimated by comparing mean annual temperature differences using the formula

$$Z = \frac{T_{sealevel} - T_{high}}{\gamma_t}, \qquad (8)$$

where $\gamma_t$ defines an empirical coefficient relating surface temperature linearly to elevation, the terrestrial lapse rate, and is usually chosen to agree with the local climate (Axelrod, 1966; Wolfe and Schorn, 1989; Gregory and Chase, 1992). Meyer (1992) calculated local $\gamma_t$ for 39 areas of the world with surface topography greater than 750 m and found $\gamma_t = 5.9 \pm 1.1$ K/km, but has a range from 3.64 to 8.11 K/km. Wolfe (1992) showed that regionally averaged values of $\gamma_t$ calculated from mean annual temperatures at high altitudes and at sea level at the same latitudes vary over a range of 3 to 9 K/km.

In using mean annual temperatures, one implicitly assumes the longitudinal invariance of the surface distribution of a quantity $G = T + \gamma_t Z$ (bottom of Fig. 3). For $\gamma_t = 5.9$ K/km, we calculated deviations from longitudinal invariance of *G* to be 3.2 K for the present climate. Hence, a minimum standard error, $\sigma_z$, for estimating altitude can be computed from these results, using

$$\sigma_z^2 = \frac{\sigma_G^2 + \sigma_T^2}{\gamma_t^2} + \frac{(\Delta T)^2 \sigma_{\gamma_t}^2}{\gamma_t^4}, \qquad (9)$$

where $\sigma_G$ and $\sigma_{\gamma_t}$ are the standard errors of *G* and $\gamma_t$, respectively. With the inclusion of an uncertainty in $\gamma_t$ of 1.1 K/km (Meyer, 1992), minimum uncertainties in the estimated altitudes increase with altitude: standard errors are 540 m, 660 m, and 920 m for altitudes of 0 m, 2000 m, and 4000 m, respectively. Hence, even ignoring the unpredictable temporal changes in $\gamma_t$ over geologic time, these estimates of minimum uncertainties exceed that of 460 m from assuming longitudinal invariance in *h*. We note that Wolfe and Schorn (1994) and others (e.g., Gregory, 1994) have typically used lower values of $\gamma_t$ for the warm periods such as Eocene time. This implies that the error due simply to an uncertainty in $\gamma_t$, $(\Delta T)\sigma_{\gamma_t}/\gamma_t^2$, will reach 1500 m with $\gamma_t = 3$ K/km for a 4-km-high mountain, and the overall altitude error, $\sigma_z$, will increase for higher estimates of altitude.

We suspect that the variations in $\gamma_t$ from 3 to 9 K/km, determined by Meyer (1986, 1992) and Wolfe (1992), are consistent with approximately longitudinal invariance of *h* and large variations in *q*. Differentiating equation 1 with respect to *Z* while holding *h* constant yields

$$-\frac{\partial T}{\partial Z} = \left(g + L_v \frac{\partial q}{\partial Z}\right)\frac{1}{c_p'}. \qquad (10)$$

Because air cools adiabatically as it rises, and because *q* depends strongly on *T* (at saturation), *q* will not be conserved as an air mass rises over high terrain. Condensation and precipitation reduce *q*, but conservation of *h* requires that at a constant pressure, *T* increases when condensation occurs. Thus, in such regions like the Sierra Nevada, vertical gradients of specific humidity directly determine the vertical temperature gradients. In that region, surface temperatures decrease slowly with altitude, at only 3 K/km (Wolfe, 1992). Regardless of whether conservation of *h* can account for other large variations in *q*, clearly *H*, instead of *T*, should be used to estimate elevation changes, at least insofar as mean annual enthalpy can be inferred well from paleobotanical material.

**Relevant Paleobotanical Work**

A major goal of paleobotany is to quantitatively estimate the climatic environment of a paleoflora. To achieve this goal, one first distinguishes the various taxa represented by the fossil assemblage. The research presented here does not address problems associated with this task and assumes that distinctions among taxa can be made. (Note that there is no need to identify taxa, just to recognize different taxa.) Second, one identifies features of the paleoflora that are related to the local climate. The method chosen here uses the character states of leaf size and shape for the flora to make the distinctions and to estimate the mean climate. Before proceeding to quantify the relation between leaf character states and climate, we briefly discuss other methods based on physiognomy for estimating paleoclimate.

**Previous Physiognomic Methods for Estimating Paleoclimate.** Previous work has shown that foliar physiognomy correlates with climatic parameters, such as mean annual temperature or growing season precipitation, suggesting that we

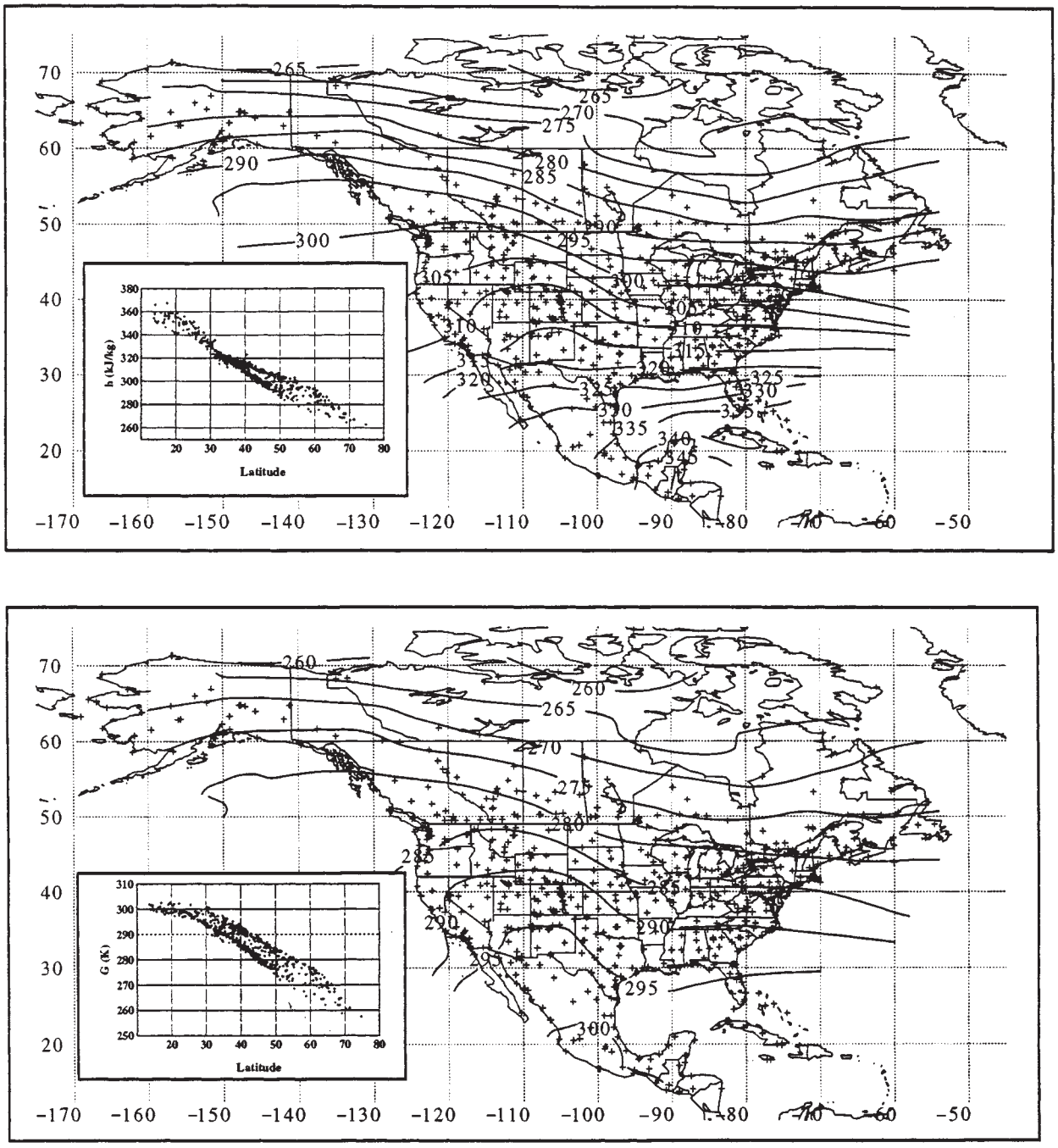


**Figure 3. (Top) The spatial distributions of mean annual moist static energy. The station locations are presented as crosses to indicate the spatial coverage of the data set. The distribution of mean annual moist static energy as a function of latitude is also shown (insets). (Bottom) The spatial distribution of the function $G = T + \gamma_t Z$ along with $G$ vs. latitude, where $T$ is the mean annual temperature, $Z$ is the station elevation, and $\gamma_t$ = 5.9 K/km.**

might expect to predict mean annual enthalpy through similar techniques. Bailey and Sinnot (1915, 1916) first described a relationship between the fraction of species with smooth margins of leaves and mean annual temperature. Wolfe (1971, 1979) and Wolfe and Hopkins (1967) refined this relationship showing that a change of 32% entire-margined species corresponds approximately to a 10 K change in mean annual temperature. Wolfe (1971) and Wolfe and Hopkins (1967) used this relationship to infer a history of mean annual temperature for northwest North America that revealed a sharp drop in temperatures separating the Eocene and Oligocene Epochs, which Shackleton and Kennett (1975) later recognized in variations of oxygen isotopes in marine microorganisms. Because of other correlations between foliar shape and living environment (Givnish, 1987), Wolfe (1993) expanded the list of characteristics to include other foliar shape parameters: size, apex and base shape, lobedness, and overall shape. With these additions, he developed the Climate-Leaf Analysis Multivariate Program (CLAMP) utiliz-

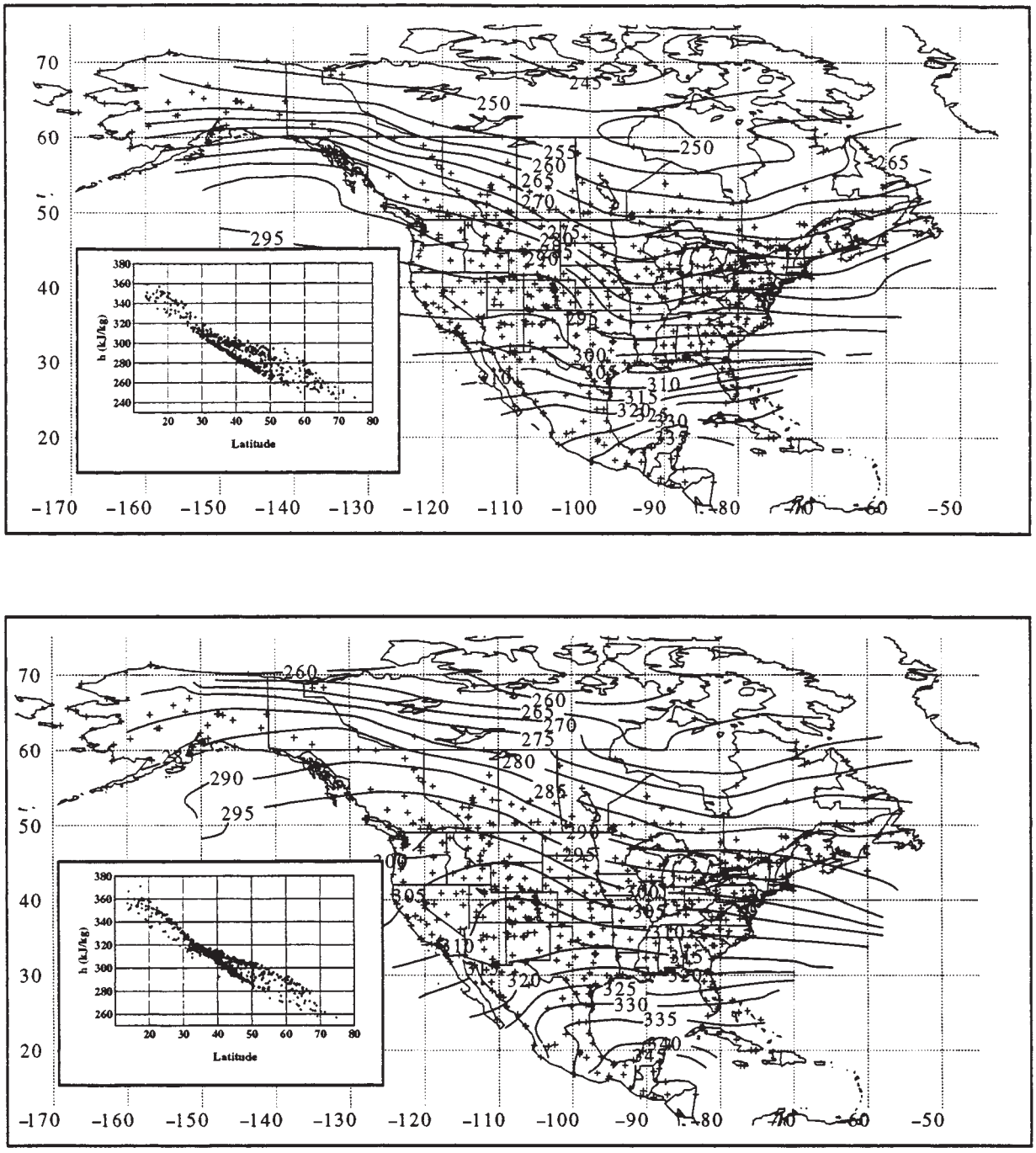


**Figure 4. Same as top of Figure 3, except for winter (top) and spring (bottom) seasons.**

ing correspondence analysis (Wolfe, 1993) to determine the relation between climate and leaf shapes and sizes. Others have also employed multivariate regression techniques using the CLAMP data to infer paleoclimate parameters (Wolfe, 1990; Gregory, 1994; Gregory and Chase, 1992; Forest et al., 1995; Greenwood and Wing, 1995).

Although quantitative theories cannot account for the character states of leaves, sufficient work demonstrates that physical processes and properties are qualitatively responsible for leaf morphology systematically varying with environmental factors. The physiognomic relation to environment should be "robust in space and time because it is controlled primarily by the physical laws of gas diffusions, fluid transport, and evaporation" (Herman and Spicer, 1996, p. 330). This suggests that observed relationships between physiognomy and climate are unlikely to result from coincidence and probably reflect patterns that existed in the past.

### Estimating Paleoclimate

The task remains to determine the mean annual enthalpy from plant physiognomy. We present an analysis relating foliar physiognomic character states to mean annual values of enthalpy, temperature, specific humidity, and rela-

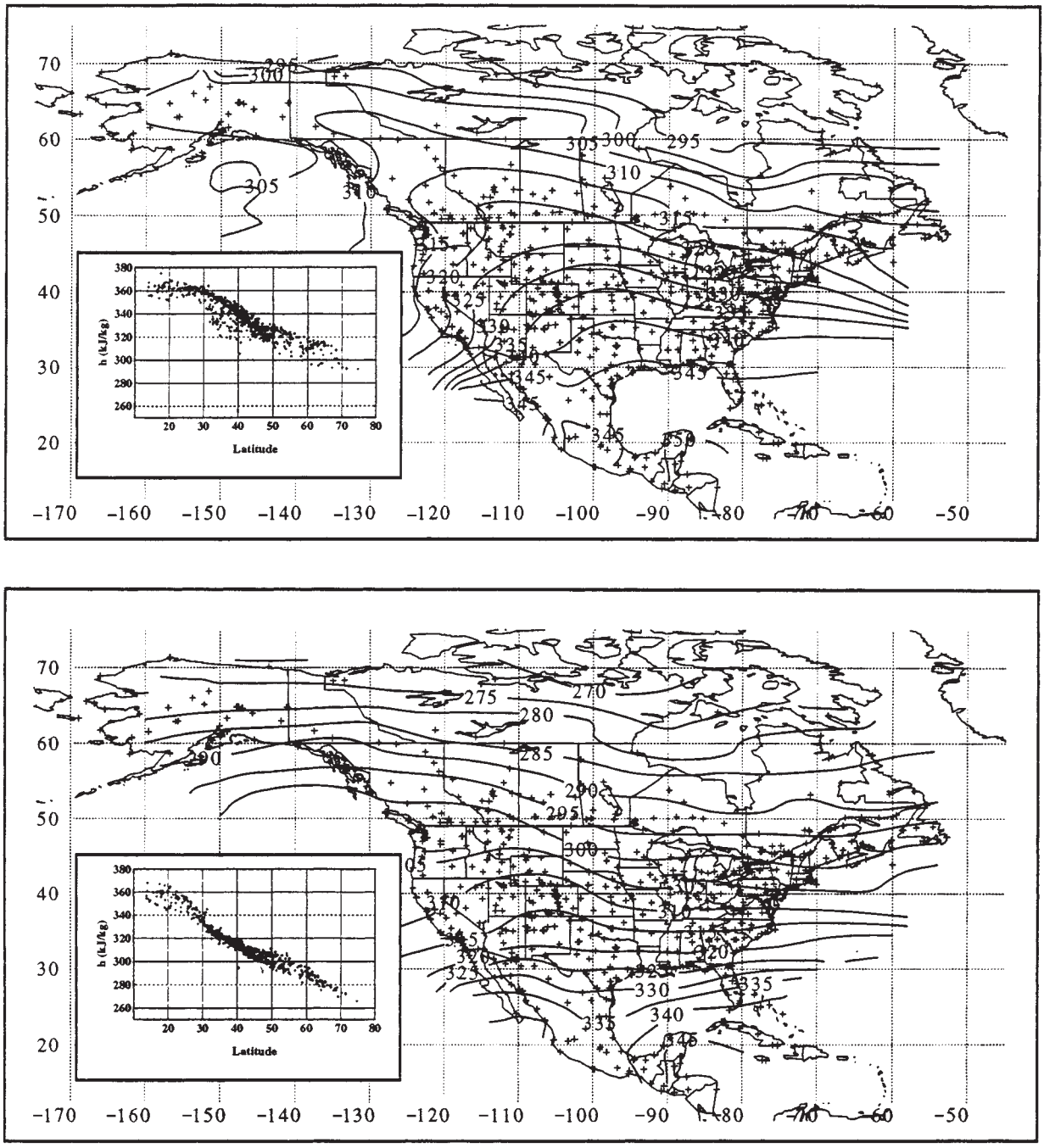


**Figure 5. Same as top of Figure 3, except for summer (top) and autumn (bottom).**

tive humidity that exploits the method and data in the CLAMP (Wolfe, 1993). From present-day plant data collected from North America, Puerto Rico, and Japan, we searched among leaf parameters for linear combinations of the foliar character states that covary with the local climates. By doing so, we determine which foliar character states covary with one another and which best correlate with climate parameters.

**Data.** To extract climate information (e.g., mean annual temperature, precipitation, specific humidity, or moist enthalpy) from fossil flora, one must first determine which typical foliar character states of extant plants show relations to present-day local climate. For forests in well-characterized climates, Wolfe (1993) measured average character states of foliar physiognomy, weighting each taxon equally (otherwise, taxa are ignored). For each taxon, the character states of its representative leaves were identified and recorded. The character states can be separated into seven categories (see Tables 5 and 6 and Fig. 6). For each vegetation site, the numbers of displayed character states for all represented species were totaled and the percentages of species exhibiting a given character state were calculated. This percentage was called the score of the leaf character state for a given site. (See Wolfe [1993] for the method of calculating character state scores.) In all, Wolfe (1993) scored leaf samples for 29 leaf character

states, using 123 vegetation sites distributed across the Northern Hemisphere, of which 112 are in North America, 9 are in Puerto Rico, and 2 are in Japan. The data presented here include two additional size categories, making the total 31 character states. The sites were chosen to be near meteorological stations to obtain measurements of temperature and precipitation, but most stations did not record humidity (see following).

Wolfe (1993) estimated that at least 20 separate taxa are necessary to infer climate parameters reliably. We can understand this estimate by relating the number of taxa to a possible source of error in the score data and comparing the error to some measure of information content in the data. If $N$ were the number of taxa for an assemblage and a single miscount or improper identification were the source of error, then the error in the score would be $1/N$. We want this error to be much less than typical variations of the scores. The standard deviations for each foliar characteristic have a mean of 9.9%, and this mean represents an average difference in leaf scores between vegetation sites for all characteristics. Thus, we require that $1/N << (\ 0.099$ or $N>>10$ and note that 20 marginally satisfies this relationship. Povey et al. (1994) corroborated this estimate by using the CLAMP (Wolfe, 1993) to infer paleotemperatures from random subsets of data from a particularly rich fossil assemblage containing 150 taxa. They found that at least 20 taxa were necessary for a subset of taxa to yield an estimate of the mean annual temperature within 2.0 °C of the estimate using 150 taxa, and that little was gained with additional taxa if $N > 30$. In Povey et al. (1994), the range of estimates decreases from ~10 °C to 4 °C when the number of taxa sampled increases from 10 to 20. Thus, a clear improvement in the accuracy is gained by requiring $N \geq 20$.

Present-day environmental data are also required for the leaf collection sites. Because humidity data are not available for each vegetation site, we could not directly calculate mean enthalpy for all sites. Instead, we used data from the meteorological stations (Fig. 3) and interpolated moist static energy to the vegetation sites. For the same reasons that we expect $h$ to be longitudinally invariant, we expect $h$ to be a smoothly varying field. Hence, the local variability of $h$ should be small over dimensions of mountains and valleys. Having a nongridded data set, we followed meteorological methods (Barnes, 1964) and interpolated from nearby stations using a distance-weighted mean,

$$h_{plantsite} = \frac{\sum_i h_i w_i}{\sum_i w_i} \qquad (11)$$

where $w_i = \exp([r_1/d]^2)$, $r_i$ = radial distance from plantsite to the meteorological station $i$, and $d$ is the average distance to the nearest station, 90.8 km. Knowledge of the elevation, $Z$, and mean annual temperature, $T$, at the vegetation sites allows the calculation of mean moist enthalpy, $H = h - gZ$, and specific humidity, $q = (H - c_p'T)/L_v$, from the interpolated value of $h$. Using data from 123 sites, we sought correlations of the 31 leaf character states with moist enthalpy and also, separately, with mean annual values of temperature, specific humidity, and relative humidity.

**Data Analysis.** The relation between leaf physiognomy and climate parameters has been analyzed by Canonical Correspondence Analysis (CANOCO) (see ter Braak, 1986; ter Braak and Prentice, 1988), a form of direct gradient analysis. Predicting climate parameters from foliar physiognomic character states follows a technique analogous to that used by ecologists to relate species to environment (see the review by ter Braak and Prentice, 1988). Fundamentally, two tasks exist in this type of research: (1) the removal of redundant information from the foliar physiognomic data, and (2) the estimation of a robust relation between the climate parameter and physiognomic data. Traditionally, one removes redundant information (Fig. 7) by identifying combinations of foliar data that vary together and thereby creating new variables that capture the gross variations of the physiognomic data. Following the ecological community's terminology, this procedure is called ordination and includes methods such as principal components

TABLE 4. ZONAL VARIABILITY OF MOIST STATIC ENERGY (in kJ/kg)

| Period | Winter | Spring | Summer | Autumn | Annual |
|---|---|---|---|---|---|
| $h_{max}$ | 6.96 | 5.74 | 6.03 | 4.21 | 5.05 |
| $h_{mean}$ | 6.80 | 5.15 | 5.44 | 3.79 | 4.48 |
| $h_{min}$ | 6.93 | 4.92 | 5.28 | 3.96 | 4.33 |

TABLE 5. FOLIAR CHARACTERISTICS*

| Characteristic | Number of categories | Description |
|---|---|---|
| Lobed | 1 | |
| Margin shape | 6 | No teeth, regular, close<br>Round, acute, compound |
| Leaf size | 9 | Nanophyll; leptophyll I ,II;<br>microphyll I, II, III; mesophyll I, II, III |
| Apex shape | 4 | Emarginate, round<br>Acute, attenuate |
| Base shape | 3 | Cordate, round, acute |
| Length to width ratio | 5 | <1:1, 1–2:1, 2–3:1, 3–4:1, >4:1 |
| Leaf shape | 3 | Obovate, elliptic, ovate |

*See Figure 6 for examples.

TABLE 6. SPECIFICATION OF FOLIAR SIZE CATEGORIES

| Size category | Leaf area ($mm^2$) |
|---|---|
| Nanophyll | <5 |
| Leptophyll I | 5–25 |
| Leptophyll II | 25–80 |
| Microphyll I | 80–400 |
| Microphyll II | 400–1400 |
| Microphyll III | 1400–3600 |
| Mesophyll I | 3600–9000 |
| Mesophyll II | 9000–15000 |
| Mesophyll III | >15000 |

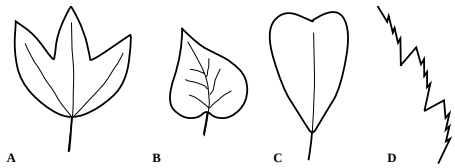


**Figure 6. Sketches of representative leaves showing various leaf character states. (A) A lobed leaf with an acute apex, a round base, and no teeth (as in B and C). (B) An ovate leaf with an attenuated apex (drip tip) and a cordate base. (C) An obovate leaf with a round and emarginate apex, and an acute base. (D) A leaf margin with teeth that are compound, acute, closely spaced, and regularly spaced (after Wolfe, 1995).**

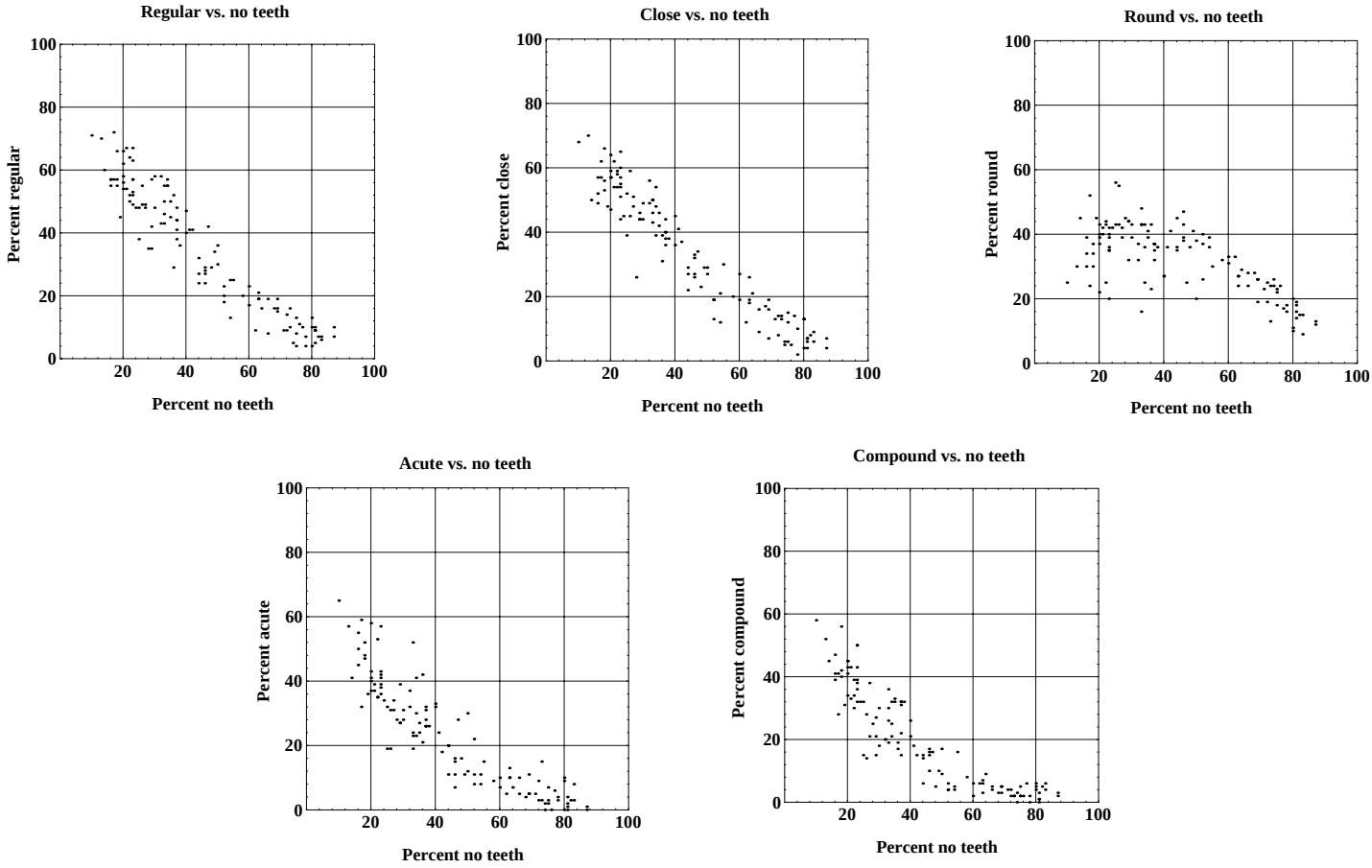


**Figure 7. The correlations of the no-teeth parameter with the other teeth character states are displayed to show the interdependent nature of the untransformed foliar character state variables. We compare this with Figure 10.**

analysis and principal correlation analysis. The new variables define a set of axes along which the gross changes in foliar data can be plotted. One can think of this as a transformation or compression of information into a reduced set of linearly independent variables that capture the internal variability of the foliar data. The second task is a calibration procedure where the new physiognomic variables are used to predict the climate parameters. Standard linear regression is an example of a calibration procedure.

The combination of ordination and calibration is called gradient analysis and has two common forms. Treating the two tasks as separate processes, indirect gradient analysis involves the use of some ordination technique before the regression relation is found. Thus, indirect gradient analysis does not make use of the climate information during the ordination procedure. Direct gradient analysis performs the two tasks simultaneously and therefore uses the climate parameters during the ordination procedure. CANOCO is a direct gradient analysis method and is distinguished from other similar methods (e.g., canonical correlation analysis) by its method of ordination. Rather than assuming a linear relation between physiognomic characters and climate parameters, canonical correspondence analysis, like its counterpart correspondence analysis, assumes that the distribution of foliar characteristics along the environmental gradient is nonlinear. Specifically, CANOCO assumes that the relation is given by a segment of the relation $y \alpha \exp(-x^2/\rho^2)$ where $y$ is the physiognomic variable, $x$ is the score along the environmental ordination axis, and $\rho$ determines the width of the Gaussian shaped curve.

CANOCO yields two sets of information, physiognomic and environmental axes as well as the associated variance explained by each axis. Each axis represents a weighted linear combination of the physiognomic scores or environmental parameters that explains a certain amount of variance in the given data. The method chooses the first axis by determining the direction in physiognomic data space that maximizes the variance explained in the environmental parameter data. Simultaneously, it chooses a direction in environmental parameter space that maximizes the variance explained in the physiognomic data. Subsequent axes for respective data sets are chosen to explain a maximum in the remaining unexplained variance. Because of these relations, the environmental and physiognomic data sets can be projected onto their respective principal axes to make a single plot.

To understand the relative importance of each axis, the variance explained by a given axis is determined from the associated eigenvalues. The percentage of variance explained is calculated as the ratio of a given eigenvalue to the sum of all eigenvalues. In this manner, the percentage of variance explained by a given set of axes can be calculated and is a measure of the information content of a given axis. Overall, the eigenvalues can be used to determine the useful information content. Typically, a change in slope on the plot of $\log(\lambda_i)$, where $i$ is the index of the eigenvalues, indicates a cutoff location where information contained in the axes beyond this index is questionable due to noise contamination (Mardia et al., 1979).

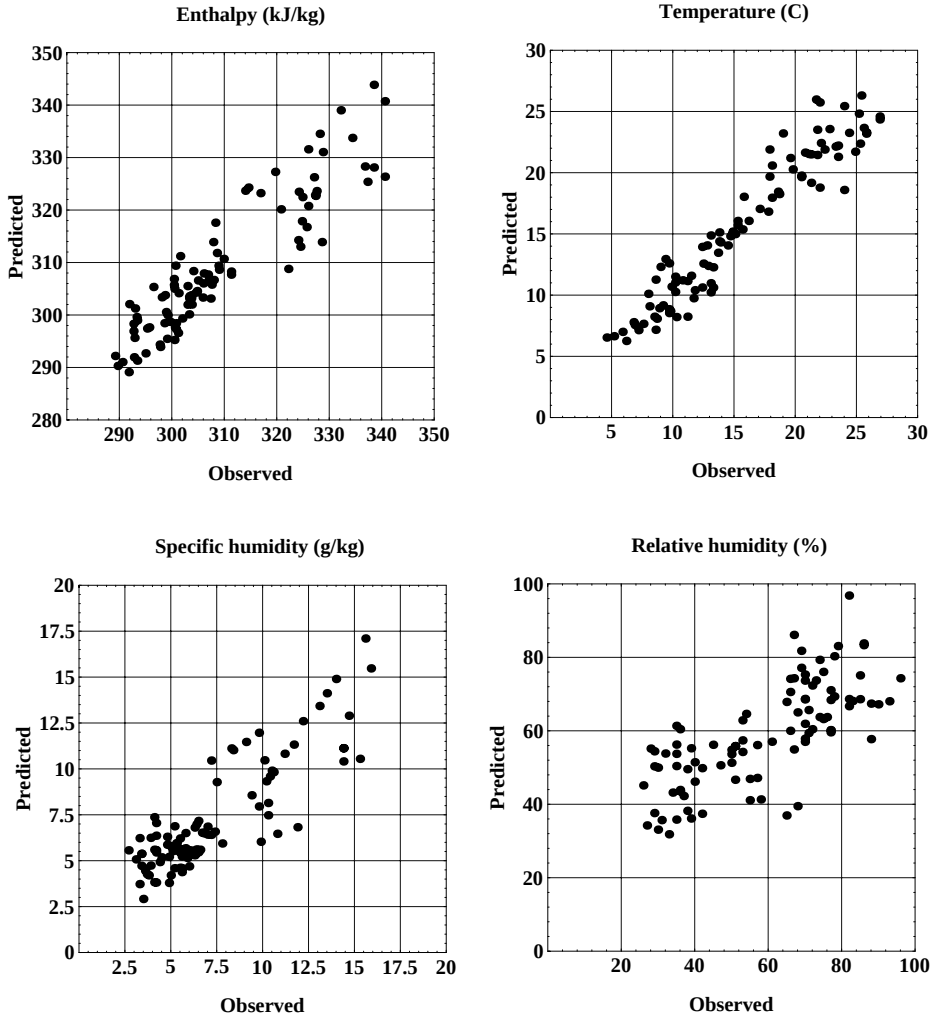


**Figure 8. The predictions of the climate parameters from the plant character state variables as given by canonical correspondence analysis are plotted vs. the observations for the plant collection sites for mean annual enthalpy (kJ/kg), temperature (°C), specific humidity (g/kg), and relative humidity.**

The estimate of a climate parameter is obtained by projecting the physiognomic scores of a given sample onto the vector obtained for the climate parameter. The value of the climate parameter is plotted against the value of the projection onto the climate vector in the physiognomic space. A least-squares fit is obtained and provides a predictive formula for the given climate parameter (see Wolfe, 1995).

**Results of Physiognomy-Climate Analysis.** From the CLAMP data and associated mean annual climate data, we obtained estimates of enthalpy, temperature, relative humidity, and specific humidity (Fig. 8). The data set was reduced by removing the outliers as indicated by scores along the third and fourth axes (see Wolfe, 1995, for a description). The axis eigenvalues from CANOCO indicate that significant information is contained in the first six axes (Fig. 9) and implies that the use of axes three and four as an outlier indicator should be robust. The estimates of the climate data indicate that mean annual enthalpy can be predicted from fossil leaf physiognomy with an uncertainty of $\sigma_H$ = 5.5 kJ/kg. In addition, the standard errors for the estimates of temperature, specific humidity, and relative humidity are respectively, $\sigma_T$ = 1.8 °C, $\sigma_q$ = 1.7 g/kg, and $\sigma_{RH}$ = 13%.

The interpretation of the projected scores along the given axes is simplified because CANOCO transforms both the environmental and physiognomic data onto the same axes (see Fig. 10). These projected scores create vectors that provide visual aids for comparisons between climate parameters. The total length of a climate parameter vector indicates the relative importance for explaining variations in the physiognomic data set. The vector length along a given axis (i.e., the direction) signifies the relative importance of the climate parameter for constraining that axis.

The mean annual temperature vector is the longest and aligns most closely with the first axis, signifying that mean annual temperature explains more overall variations in the physiognomic data than any other climate variable. Because the temperature vector aligns more with the first axis than do the other variables (see Fig. 10), the first axis is referred to as the temperature axis. The relative humidity and specific humidity vectors enclose the second axis and accordingly, the second axis is referred to as the moisture stress axis. The enthalpy vector projects roughly equally onto the first and second axes, indicating that enthalpy contains relevant information regarding both temperature and moisture, as anticipated. These associations allow us to infer which character states are most important for estimating the climate parameters discussed in the following.

The relative directions of the four climate parameter vectors are explained by the physical relation between them. First, the temperature vector is nearly orthogonal to the relative humidity vector. This is consistent with relative humidity being a departure from saturation conditions, which should be nearly independent of temperature. Second, the specific humidity is midway between the relative humidity and temperature vectors. Because the specific humidity is a measure of the total water vapor content of the air, it should be correlated with both temperature and the relative humidity, as shown. Last, the enthalpy vector is between both specific humidity and temperature, which follows from the definition of enthalpy as the combined specific and latent heat energies.

The projections of the physiognomic characteristics onto a given axis represent the relative importance of the characteristics for explaining the environmental variations along that axis. The first axis (Fig. 11), which is strongly related to mean annual temperature, has significant contributions from the entire margin (2) (i.e., no teeth), small leaf sizes (8–10), and emarginate apex character states (17). In contrast to this, the second axis, related to moisture stress, has contributions from the large leaf sizes (13–16), attenuate apices (20), and long narrow leaves (28).

Because estimates of mean annual temperature, specific humidity, and relative humidity are determined independently, an alternative estimate of the mean annual enthalpy can be calculated by combining the respective energy components. To use the relative humidity estimate to

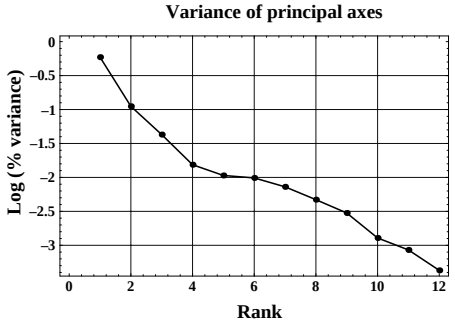


**Figure 9. Logarithm of normalized eigenvalues calculated from the covariance matrix of present-day leaf physiognomy data. The eigenvalues represent the variance explained by each eigenvector in the foliar physiognomy data set.**

obtain a specific humidity, we use the mean annual temperature estimate and the definition of relative humidity to write

$$q = \varepsilon RH \frac{e^* T}{p - (1-\varepsilon) e^*(T)}$$

(see preceding). We note that estimating these parameters separately does not improve the estimate of enthalpy because

$$\sigma_H^2 = \left(c_p' \sigma_T\right)^2 + \left(L_v \sigma_q\right)^2 + 2c_p' L_v \sigma_T \sigma_q r(T,q)$$

or (12)

$$\sigma_H^2 = \left(c_p' \sigma_T\right)^2 + \left(\frac{\varepsilon L_v}{p}\right)^2 \left\{\left[\sigma_{e^*(T)} RH\right]^2 + \left[\sigma_{RH} e^*(T)\right]^2\right\},$$

where $\sigma_T$, $\sigma_q$, $\sigma_{RH}$, and $\sigma_{e^*(T)}$ are the standard errors of the respective variables; and $r(T,q) = 0.80$ is the correlation coefficient between $T$ and $q$, and $\sigma_{e^*(T)}$ is the standard error of the saturation vapor pressure, which is a function of $T$ and $\sigma_T$. This yields a standard error, $\sigma_H = 5.8$ kJ/kg, which is larger than the error for calculating $h$ directly from foliar data.

The contribution to the total error from the uncertainty, $\sigma_H = 5.5$ kJ/kg, in predicting mean annual enthalpy is 560 m. We estimate a comparable error, 390 m with $\gamma_t = 5.9$ K/km, for the mean annual temperature approach. This latter error is clearly an underestimate, because it is dependent on the choice of $\gamma_t$, whereas the former error will remain constant.

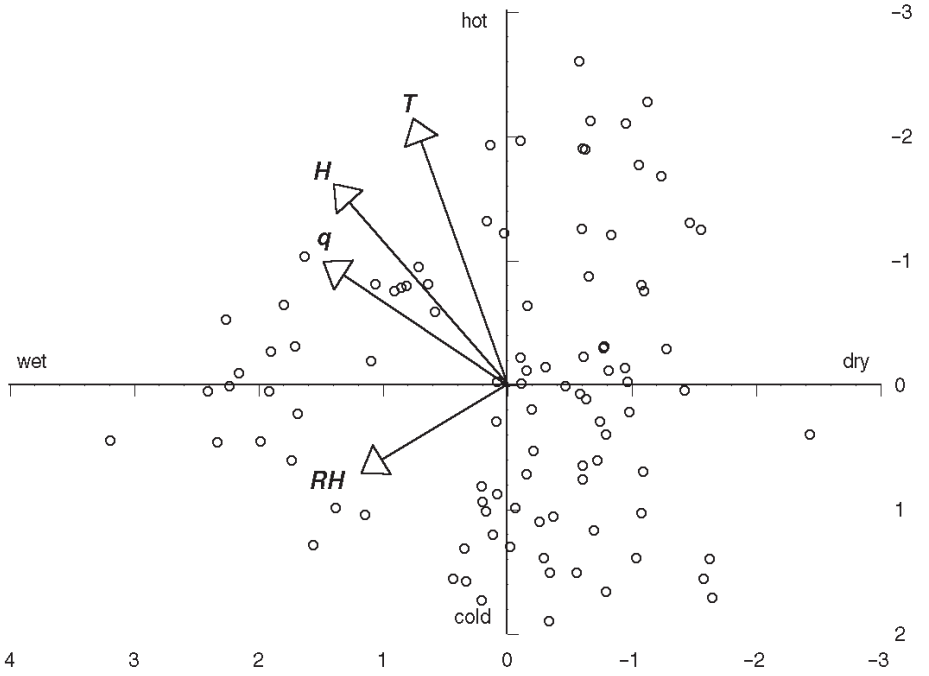


**Figure 10. The projections of the physiognomic scores onto the first (vertical) and second physiognomic axes are plotted for the leaf collection sites. The environmental vectors represent the correlation of the given parameter with the directions of the principal axes (after Wolfe, 1995). See Table 1 for symbols.**

### Total Expected Error in Paleoaltitude

We obtain an expected error for the paleoaltitude by combining the expected errors from the zonal asymmetry, $\sigma_h = 4.5$ kJ/kg, and from the botanical inferences of enthalpy, $\sigma_H = 5.5$ kJ/kg, at each location.

$$\sigma_z = \sqrt{\frac{2\sigma_H^2 + \sigma_h^2}{g^2}} = 910 \text{ m} \qquad (13)$$

where the errors in enthalpy from sites at sea level and inland have been combined to yield the factor of two. Other quantifiable sources of error could be included in a similar manner.

We can also estimate the standard error in altitude by predicting the altitude of the present-day plant-collection sites. We assume that the sea-level enthalpy follows a linear function of latitude based on the latitudinal distribution of moist static energy. Restricting our data to latitudes south of 55°N, where our assumption of zonal symmetry is valid, the standard deviation of the predicted altitude is 620 m (see Fig. 12). We believe that this small scatter results partly from the use of altitude to estimate enthalpy at plant sites for which we have no humidity data. For such sites, we relied on meteorological estimates of $h$ and heights of sites to infer $H$, causing an unavoidable dependence of the value of $H$ on altitude. The lower error estimate of 620 m implies that the error estimate of 910 m calculated from expected errors in the components is robust.

We discuss some potential sources of error related to taphonomic, microclimatic, and fossil dating considerations, which are difficult to quantify for a paleoaltitude estimate. Taphonomic processes, the processes affecting the deposition of fossils, might affect the fossil flora either by transporting leaves from nonlocal flora or by favoring preservation of certain leaves or leaf characteristics. Studies of taphonomy suggest that transport of leaves is ~1 km or less (Spicer and Wolfe, 1987; Spicer, 1989), making it unlikely that representatives from a different climate would be intermixed in a fossil assemblage. Transport before fossilization, however, might affect leaf distribution, for example, by eliminating fragile specimens or by damaging them so that they appear to be different taxa. For example, Wolfe and Schorn (1989) identified 33 species represented in the Oligocene Creede flora, whereas Axelrod (1987) identified 73 species from the same fossil assemblage. This difference

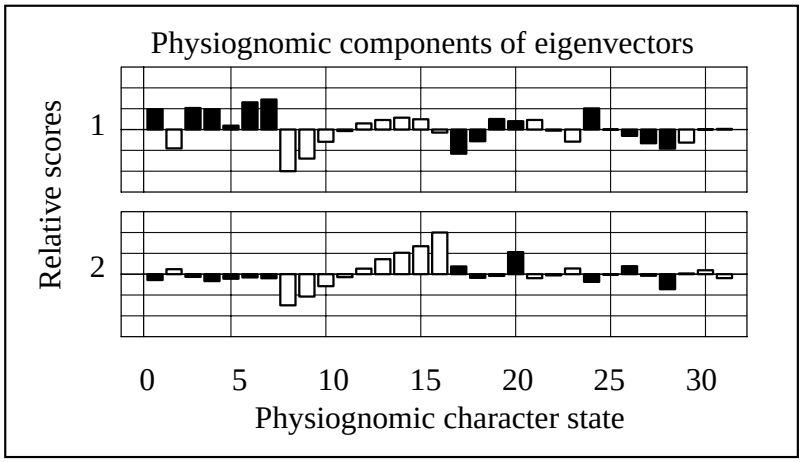


**Figure 11. Normalized components of the first two eigenvectors of the canonical correspondence analysis show the relative contributions from the 31 leaf character states. The order of the character states corresponds to that in Tables 5 and 6. The components are normalized by each vector's maximum value (not the eigenvalue), which are 1.08 and 0.88, respectively. Within each vector, the values represent the individual contribution by each character to the overall signal.**

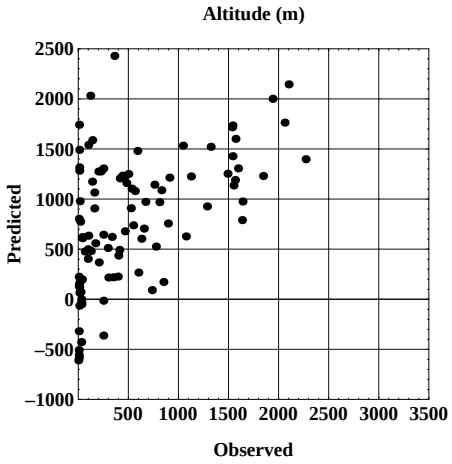


**Figure 12. The predicted altitude for the plant collection sites plotted against the true altitude of the sites.**

calls attention to the need for careful analysis and to a potential error that we cannot easily quantify. There is also some risk that the size distribution of leaves in litter beneath a tree will differ from that growing on it (Spicer, 1989; Greenwood, 1992). Gregory (1994) corrected for such sorting in her scoring of one fossil assemblage.

A bias from a high-energy deposition process must also be considered. This will result in larger leaves being destroyed as well as small features being removed from the leaves. Specifically, teeth and apices can be destroyed in the deposition process. One feature of CLAMP is that the leaves were collected near stream-side environments where possible and thus should represent the leaf sample entering streams and reaching lake sediments. Although this does not remove the bias from the fossil record, it does bias the size distribution of the present-day data in a similar manner.

Because fossil assemblages can be scored from fossil collections or from illustrations of fossils in the literature, incomplete collections or displays can lead to biased estimates of the physiognomy of a flora. For example, if a flora is scored from a full fossil collection, fragments of fossils can be used to improve estimates of scores such as teeth and apex characteristics. These characteristics are easily destroyed in a high-energy depositional environment; however, their scoring can be amended by using fossil fragments provided the taxa can be properly identified. Hence, if a flora were scored from the literature and fragments were not displayed, the physiognomic scores are considered less reliable than those from full collections or more complete presentations in the literature.

Because we require two isochronous floras to estimate a paleoaltitude, we must account for errors in the dating of fossil floras. Dating of fossil floras is accomplished by radiometric dating of minerals in strata near the fossil deposition beds or stratigraphic dating based on known correlations between stratigraphic properties such as isotopes, magnetic properties, or index fossils. Error estimates of radiometric ages can be as low as ±0.005 m.y. (Swisher, 1992) for the $^{40}Ar/^{39}Ar$ dating technique. Error estimates for the K/Ar technique can be ±0.5 m.y. This method was commonly used until the development of the $^{40}Ar/^{39}Ar$ technique. In cases where no radiometric age is available, dating errors can be several million years.

To account for dating errors in a paleoaltitude estimate, we must estimate the variability of climate on time scales shorter than the time scale associated with a dating error. We might look for an upper bound by examining the climate variability of the Pleistocene Epoch (0–1.6 Ma). During this period, the major changes in climate occurred on time scales of 10–100 k.y., during which the Northern Hemisphere continental ice sheets grew and decayed and global mean temperature changed 2–3 °C. In mid-latitude regions where we would estimate paleoaltitudes, temperature changes were perhaps 5–10 °C (Crowley and North, 1991) between glacial and interglacial climates. These temperature differences present an upper bound on the variability of climate for these regions because prior to Pliocene time (ca. 5 Ma), large-scale glaciation was limited to Antarctica (Crowley and North, 1991). To conceive of temperature changes as large as differences between the interglacial and glacial climates, we would require an equally large change in a climate-forcing parameter such as the albedo. For this reason, the climate variability for pre-Pliocene time most likely was smaller than the observed climate variability during Pleistocene time. Supposing a maximum additional random error of 5 kJ/kg for short time-scale variability that corresponds to 2.5–3 °C temperature differences, and associated differences in $q$, the paleoaltitude error would be 1000 m.

There is a risk that the plants affect the microclimates in which they grow, for example, by maintaining a more humid local environment than in the air nearby and above. To some extent such an effect will apply to both present-day and ancient climates. Moreover, because we use moist static energy, such a difference in moisture will be partially compensated for by differences in temperature. In any case, the potential errors associated with transport of leaves, fossil dating, and local variations in climate are reminders that we should expect modifications and improvements in the approach taken here.

## SUMMARY AND CONCLUSIONS

We have presented a method for estimating paleoaltitudes based on comparing the local paleo-

climate from some elevated region to that at sea level and at approximately the same latitude. Rather than comparing mean annual temperatures as others have done to obtain $Z$, we compare moist enthalpies, which is equivalent to assuming the invariance of moist static energy, $h$, between locations. This approach differs significantly from previous methods by incorporating the effect of moisture on the temperature distribution. During condensation processes, the latent heat of vaporization is released and subsequently warms the air. To estimate a paleoaltitude, we require that $h$ be invariant between fossil sites and that the moist enthalpy, $H$, be inferable from fossil plant leaves. We tested these requirements by examining the present-day climatic and foliar data to quantify the expected errors for the method.

We first examined the present-day distribution of climatic values of $h$ at the surface for the four seasons plus the annual mean to show that mean annual $h$ is approximately invariant with longitude and altitude. The surface distribution results from two properties of atmospheric flow: conservation of $h$ following the large-scale flow and the maintenance of the vertical profile of $h$ by convective processes. Using monthly mean data, we examined the distribution and calculated the expected error from assuming zonal invariance to be 4.5 kJ/kg for the mean annual climate. This error translates to an altitude error of 450 m and is compared with an equivalent error of 500 m from the mean annual temperature approach. Moreover, the uncertainty of the terrestrial lapse rate, $\gamma_t$, increases the expected error in elevation as elevations increase, particularly when small lapse rates are assumed.

To estimate paleoenthalpy from plant fossils, we quantified a relationship between leaf physiognomy and enthalpy from present-day plants and their local climate. Using canonical correspondence analysis, we can estimate mean annual enthalpy with an uncertainty of 5.5 kJ/kg. The contribution to the uncertainty in altitude is 560 m and is comparable to using temperature alone. The results indicate that lobedness, teeth, size, and apex characteristics are all important for estimating enthalpy. We also found uncertainties of 1.8 °C, 1.7 g/kg, and 13% for mean annual temperature, specific humidity, and relative humidity, respectively. These climatic variables can be used as alternative estimates of enthalpy but do not necessarily reduce the expected error in altitude. Other statistical techniques that improve the ability to estimate enthalpy could replace the current method.

To apply our method to a paleoclimate problem, we tacitly assume that the errors as estimated from today's climate and plants are similar to those of the past. Taphonomic processes involved in the deposition of plant fossils appear not to affect our climate estimates. Combining the estimated uncertainties indicates an altitude error of 910 m. This compares favorably with altitude errors of 1100–1400 m from differences in paleopressure (Sahagian and Maus, 1994) and 800–1500 m from differences in paleotemperature.

## ACKNOWLEDGMENTS

We thank M. Raymo, P. England, R. Spicer, and L. Stranks for constructive discussions. We also thank A. Raymond and two anonymous reviewers for comments on the manuscript. This work was supported by grants from the Climate Dynamics Program in the Division of Atmospheric Sciences of the U.S. National Science Foundation and an Office of Naval Research Fellowship to Forest.

## APPENDIX. PALEOPRESSURE ESTIMATION METHODS

Sahagian and Maus (1994) presented a method for estimating paleopressures using basalt vesicularity, by comparing the average and median bubble sizes in the basalt flow from the surface and at some depth in the basalt. The variation in sizes of bubbles with depth depends on the pressure within the basalt, and hence on the atmospheric pressure, the thickness of the basalt flow, and the basalt density. Measurements of bubble sizes at two different depths can be used to infer the atmospheric pressure at the time of eruption. Sahagian and Maus (1994) reported an error of 0.1 bar, which corresponds to an altitude error of 1–1.4 km.

Because of the relatively large error associated with basalt vesicularity and the sparseness of unweathered basalt, we anticipate that Sahagian and Maus's method will be applicable to only rare localities.

Measurements of cosmogenic nuclide concentrations in exposed rock offer a second method for estimating paleopressure. Cosmogenic nuclides form by three processes: (1) spallation reactions with high-energy nucleons, (2) secondary thermal nucleon capture reactions, and (3) muon-induced reactions (Cerling and Craig, 1994). The majority of cosmogenic nuclides found in rock, including $^{3}$He, $^{10}$Be, $^{14}$C, $^{21}$Ne, $^{26}$Al, $^{36}$Cl, $^{53}$Mn, and $^{131}$Xe, are created from secondary particle fluxes from galactic cosmic rays being absorbed in the upper atmosphere and emitting neutrons toward the Earth's surface. The neutron flux reaching the surface is constrained by the mass of the atmosphere through which they pass, which in turn is directly related to the surface pressure. In addition, the magnetic field of the earth focuses cosmic rays toward higher latitudes, and thus isopleths of concentration will be an increasing function of latitude. Thus, nuclide concentrations in surface rock increase with the duration of exposure and the rate of nuclide production, which depend on latitude and altitude. Because of the relatively short half-lives of $^{10}$Be and $^{26}$Al, rock exposed to cosmogenic nuclides for long durations will reach a steady state in which radioactive decay equals production rate, and the concentration will depend only on the duration of exposure, height, and latitude.

Measured concentrations of cosmogenic nuclides from surface rock clearly can be used to test a suggested elevation history of a region. Brown et al. (1991) and Brook et al. (1995), however, used concentrations of $^{10}$Be and $^{26}$Al to place constraints on the uplift rate and duration of exposure of rocks in the Transantarctic Mountains of Antarctica. Their measured concentrations require a high terrain for a long duration because steady-state concentrations were nearly reached, and therefore disprove the suggestion that this area rose 2000 m since 2 Ma. Because of the dependence of concentration of cosmogenic nuclides on height, however, there can be no unique relationship between such concentration and the elevation history. The tightest constraint we might expect is an estimate of the mean elevation over the duration of exposure of the rock. Probably the factor that will most limit the utility of such a constraint is the difficulty in finding rock exposed for a sufficiently long duration that its elevation might have changed by several hundred meters, but during which time erosion has not exceeded as little as tens of centimeters.

Although the work of Brown et al. (1991) and Brook et al. (1995) clearly demonstrates that cosmogenic nuclides can be used to test hypotheses for recent rapid uplift, the limitations on amounts of erosion and on magnitudes of elevation change make it unlikely that such measurements will provide useful paleoaltitudes except in rare circumstances.

## REFERENCES CITED

Axelrod, D. I., 1966, A method for determining the altitudes of Tertiary floras: Paleobotanist, v. 14, p. 144–171.

Axelrod, D. I., 1987, The late Oligocene Creede flora, Colorado: University of California Publications in Geological Sciences, v. 130, 235 p.

Axelrod, D. I., and Bailey, H. P., 1969, Paleotemperature analysis of Tertiary floras: Palaeogeography, Palaeoclimatology, Palaeoecology, v. 6, p. 164–195.

Bailey, I. W., and Sinnott, E. W., 1915, A botanical index of Cretaceous and Tertiary climates: Science, v. 41, p. 831–834.

Bailey, I. W., and Sinnott, E. W., 1916, The climatic distribution of certain types of angiosperm leaves: American Journal of Botany, v. 3, p. 24–39.

Barnes, S. L., 1964, An objective scheme for interpolation of data: Journal of Applied Meteorology, v. 3, p. 396–409.

Betts, A. K., 1982, Saturation point analysis of moist convective overturning: Journal of the Atmospheric Sciences, v. 39, p. 1484–1505.

Bolton, D., 1980, The computation of equivalent potential temperature: Monthly Weather Review, v. 108, p. 1046–1053.

Brook, E. J., Brown, E. T., Kurz, M. D., Ackert, R. P. Jr., Raisbeck, G. M., and Yiou, F., 1995, Constraints on age, erosion, and uplift of Neogene glacial deposits in the Transantarctic Mountains determined from in situ cosmogenic $^{10}$Be and $^{26}$Al: Geology, v. 23, p. 1063–1066.

Brown, E. T., Edmond, J. M., Raisbeck, G. M., Yiou, F. , Kurz, M. D., and Brook, E. J., 1991; Examination of surface exposure ages of Antarctic moraines using in situ $^{10}$Be and $^{26}$Al: Geochimica et Cosmochimica Acta, v. 55, p. 2269–2283.

Cerling, T. E., and Craig, H., 1994, Geomorphology and in-situ cosmogenic isotopes: Annual Review of Earth and Planetary Sciences, v. 22, p. 273–317.

Chaloner, W. G., and Creber, G. T., 1990, Do fossil plants give a climate signal?: Geological Society of London Journal, v. 147, p. 343–350.

Crowley, T. J., and North, G. R., 1991, Paleoclimatology: New York, Oxford University Press, 339 p.

Emanuel, K. A., 1994, Atmospheric convection: New York, Oxford University Press, 580 p.

England, P., and Houseman, G., 1989, Extension during continental convergence, with application to the Tibetan Plateau: Journal of Geophysical Research, v. 94, p. 17561–17579.

Forest, C. E., Molnar, P., and Emanuel, K. E., 1995, Palaeoaltimetry from energy conservation principles: Nature, v. 343, p. 249–253.

Givnish, T. J., 1987, Comparative studies of leaf form: Assessing the relative roles of selective pressures and phylogenetic constraints: New Phytologist, v. 106, p. 131–160.

Greenwood, D. R., 1992, Taphonomic constraints on foliar physiognomic interpretations of Late Cretaceous and Ter-

tiary palaeoclimates: Reviews of Paleobotany and Palynology, v. 71, p. 149–190.
Greenwood, D. R., and Wing, S. L., 1995, Eocene continental climates and latitudinal temperature gradients: Geology, v. 23, p. 1044–1048.
Gregory, K. M., 1994, Paleoclimate and paleoelevation of the 35 Ma Florissant flora, Front Range, Colorado: Paleoclimates, v. 1, p. 23–57.
Gregory, K. M., and Chase, C. G., 1992, Tectonic significance of paleobotanically estimated climate and altitude of the late Eocene erosion surface, Colorado: Geology, v. 20, p. 581–585.
Held, I. M., 1983, Stationary and quasi-stationary eddies in the extratropical troposphere: Theory, *in* Hoskins, B., and Pearce, R., eds., Large-scale dynamical processes in the atmosphere: London, Academic Press, p. 127–168.
Herman, A. B., and Spicer, R. A., 1996, Palaeobotanical evidence for a warm Cretaceous Arctic Ocean: Nature, v. 380, p. 330–333.
Holton, J. R., 1992, An introduction to dynamic meteorology: San Diego, California, Academic Press, 511 p.
Mardia, K. V., Kent, K. T., and Bibby, J. M., 1979, Multivariate analysis: New York, Academic Press, 521 p.
Meyer, H. W., 1986, An evaluation of the methods for estimating paleoaltitudes using Tertiary floras from the Rio Grande rift vicinity, New Mexico and Colorado [Ph.D. dissert.]: Berkeley, University of California, 217 p.
Meyer, H. W., 1992, Lapse rates and other variables applied to estimating paleoaltitudes from fossil floras: Palaeogeography, Palaeoclimatology, Palaeoecology, v. 99, p. 71–99.
Murakami, T., 1987, Effects of the Tibetan Plateau, *in* Chang, C.-P., and Krishnamurty, T. N., eds., Monsoon meteorology: New York, Oxford University Press, p. 235–270.
National Climatic Data Center, 1989, International station meteorological climate summary, Volume 1: Washington, D. C., U.S. Government Printing Office, CD-ROM.
Oort, A., 1983, Global atmospheric circulation statistics, 1958–1973: National Oceanic and Atmospheric Administration Professional Paper 14, 180 p.
Peixoto, J. P., and Oort, A. H., 1992, The physics of climate: New York, American Institute of Physics, 520 p.
Povey, D. A. R., Spicer, R. A., and England, P., 1994, Paleobotanical investigation of early Tertiary paleoelevations in northeastern Nevada: Initial results: Reviews of Paleobotany and Palynology, v. 81, p. 1–10.
Raymo, M. E., and Ruddiman, W. F., 1992, Tectonic forcing of late Cenozoic climate: Nature, v. 359, p. 117–122.
Ruddiman, W. F., and Kutzbach, J. E., 1991, Plateau uplift and climatic change: Scientific American, v. 264, p. 66–75.
Ruddiman, W. F., and Raymo, M. E., 1988, Northern Hemisphere climate regimes during the last 3 Myr: Possible tectonic connections, *in* Shackleton, N. J., West, R. G., and Brown, D. Q., eds., The past three million years: Evolution of climatic variability in the North Atlantic region: Cambridge, Cambridge University Press, p. 227–234.
Sahagian, D. L., and Maus, J. E., 1994, Basalt vesicularity as a measure of atmospheric pressure and palaeoelevation: Nature, v. 372, p. 449–451.
Shackleton, N. J., and Kennett, J. P., 1975, Paleotemperature history of the Cenozoic and the initiation of Antarctic glaciation: Oxygen and carbon isotope analyses in DSDP Sites 277, 279, and 281, *in* Initial reports of the Deep Sea Drilling Project, Volume 29: Washington, D.C., U.S. Government Printing Office, p. 743–755.
Spicer, R. A., 1989, The formation and interpretation of plant megafossil assemblages, *in* Callow, J., ed., Advances in botanical research.: New York, Academic Press, p. 96–191.
Spicer, R. A., and Wolfe, J. A., 1987, Plant taphonomy of late Holocene deposits in Trinity (Clair Engle) Lake, northern California: Paleobiology, v. 13, p. 227–245.
Stull, R., 1989, An introduction to boundary layer meteorology: Boston, Kluwer Academic Publishers, 666 p.
Swisher, C. C., 1992, $^{40}Ar/^{39}Ar$ dating and its application to the calibration of the North American land mammal ages [Ph.D. dissert.]: Berkeley, University of California, 239 p.
ter Braak, C. J. F., 1986, Canonical correspondence analysis: A new eigenvector technique for multivariate direct gradient analysis: Ecology, v. 67, p. 1167–1179.
ter Braak, C. J. F., and Prentice, I. C., 1988, A theory of gradient analysis: Advances in Ecological Research, v. 18, p. 271–317.
Trenberth, K. E., and Chen, S.-C., 1988, Planetary waves kinematically forced by Himalayan orography: Journal of the Atmospheric Sciences, v. 45, p. 2934–2948.
Wallace, J. M., and Hobbs, P. V., 1977, Atmospheric science: An introductory survey: New York, Academic Press, 467 p.
Webster, P. J., and Chou, L. C., 1980, Seasonal structure of a simple monsoon system: Journal of the Atmospheric Sciences, v. 37, p. 354–367.
Wolfe, J. A., 1971, Tertiary climatic fluctuations and methods of analysis of Tertiary floras: Palaeogeography, Palaeoclimatology, Palaeoecology, v. 9, p. 27–57.
Wolfe, J. A., 1979, Temperature parameters of the humid to mesic forests of eastern Asia and their relation to forests of other regions of the Northern Hemisphere and Australasia: U.S. Geological Survey Professional Paper 1106, 37 p.
Wolfe, J. A., 1990, Palaeobotanical evidence for a marked temperature increase following the Cretaceous/Tertiary boundary: Nature, v. 343, p. 153–156.
Wolfe, J. A., 1992, An analysis of present-day terrestrial lapse rates in the western conterminous United States and their significance to paleoaltitudinal estimates: U.S. Geological Survey Bulletin 1964, 35 p.
Wolfe, J. A., 1993, A method of obtaining climatic parameters from leaf assemblages: U.S. Geological Survey Bulletin 2040, 71 p.
Wolfe, J. A., 1995, Paleoclimatic estimates from Tertiary leaf assemblages: Annual Review of Earth and Planetary Sciences, v. 23, p. 119–142.
Wolfe, J. A., and Hopkins, H. E., 1967, Climatic changes recorded by Tertiary land floras in northwestern North America, *in* Hatai, K., ed., Tertiary correlations and climatic changes in the Pacific (Symposium, Pacific Scientific Congress, 11th, Tokyo, August–September 1966, Volume 25): Sendai, Japan, Sasaki, p. 67–76.
Wolfe, J. A., and Schorn, H. E., 1989, Paleoecologic, paleoclimatic, and evolutionary significance of the Oligocene Creede flora, Colorado: Paleobiology, v. 15, p. 180–198.
Wolfe, J. A., and Schorn, H. E., 1994, Fossil floras indicate high altitude for west-central Nevada at 16 Ma and collapse to about present altitudes by 12 Ma: Geological Society of America Abstracts with Programs, v. 26, no. 7, p. A-521.
Wolfe, J. A., Schorn, H. E., Forest, C. E., and Molnar, P., 1997, Paleobotanical evidence for high altitudes in Nevada during the Miocene: Science, v. 276, p. 1672–1675.
Wolfe, J. A., Forest, C. E., and Molnar, P., 1998, Paleobotanical evidence on Eocene and Oligocene paleoaltitudes in midlatitude western North America: Geological Society of America Bulletin, in press. 1998.
Xu, K.-M., and Emanuel, K. A., 1989, Is the tropical atmosphere conditionally unstable?: Monthly Weather Review, v. 117, p. 1471–1479.
Young, J. A., 1987, Physics of monsoons: The current view, *in* Fein, J. S., and Stephens, P. L., eds., Monsoons: New York, John Wiley and Sons, p. 211–243.

MANUSCRIPT RECEIVED BY THE SOCIETY JUNE 23, 1997
REVISED MANUSCRIPT RECEIVED FEBRUARY 24, 1998
MANUSCRIPT ACCEPTED APRIL 30, 1998

Printed in U.S.A.